

Fast spin dynamics algorithms for classical spin systems

M. Krech, Alex Bunker, and D.P. Landau

Center for Simulation Physics, University of Georgia, Athens, Georgia 30602

We have proposed new algorithms for the numerical integration of the equations of motion for classical spin systems. In close analogy to symplectic integrators for Hamiltonian equations of motion used in Molecular Dynamics these algorithms are based on the Suzuki-Trotter decomposition of exponential operators and unlike more commonly used algorithms exactly conserve spin length and, in special cases, energy. Using higher order decompositions we investigate integration schemes of up to fourth order and compare them to a well established fourth order predictor-corrector method. We demonstrate that these methods can be used with much larger time steps than the predictor-corrector method and thus may lead to a substantial speedup of computer simulations of the dynamical behavior of magnetic materials.

Keywords: Heisenberg systems, Suzuki - Trotter decomposition, symplectic integrators, predictor - corrector methods, dynamic structure factor

PACS: 75.40.Mg, 75.40.Gb, 75.30.Ds, 75.40.-s

I. INTRODUCTION

Collective phenomena in many materials can be traced back to the presence of interacting magnetic moments on the atomic level. The exploration of magnetic systems therefore plays a key role in both physics and materials science. The understanding of phase transitions, critical phenomena, and scaling has in part been founded on the investigation of simple model spin systems such as the Ising, the XY, and the Heisenberg model (see below). These spin systems continue to be of high relevance for the investigation of dynamic critical behavior and dynamic scaling. On the other hand realistic models of magnetic materials can be constructed from these simple spin models, if the interaction parameters and the underlying lattice structure are taken as an input from experiments. However, in such cases the theoretical analysis of experimentally accessible quantities, such as the dynamic structure factor, is usually too demanding for analytical methods. Computer simulations of the dynamical behavior of spin systems have, therefore, become a very important tool for the theoretical understanding of dynamic critical behavior and material properties of magnetic systems, as the following examples may show.

Large scale computer simulations have been performed in recent years in order to explore the dynamical behavior of classical XY [1] and Heisenberg models [2] in $d = 2$ dimensions and of classical Heisenberg ferro- and antiferromagnets in $d = 3$ [3,4]. The simulations are based on model Hamiltonians for continuous degrees of freedom represented by a three-component spin \mathbf{S}_k with fixed length $|\mathbf{S}_k| = 1$ for each lattice site k . A typical model Hamiltonian is then given by

$$\mathcal{H} = -J \sum_{\langle k,l \rangle} (S_k^x S_l^x + S_k^y S_l^y + \lambda S_k^z S_l^z) - D \sum_k (S_k^z)^2, \quad (1.1)$$

where J is the exchange integral, $\langle k, l \rangle$ denotes a nearest-neighbor pair of spins \mathbf{S}_k , λ is an exchange anisotropy parameter, and D determines the strength of a single-site or crystal field anisotropy. For $\lambda = 1$ and $D = 0$ Eq.(1.1) represents the classical isotropic Heisenberg ferromagnet or the corresponding antiferromagnet for $J > 0$ or $J < 0$, respectively. In the case $\lambda = D = 0$ Eq.(1.1) reduces to the XY model.

Realistic descriptions of specific magnetic materials may require additional interactions in the Hamiltonian, like an additional two-spin exchange interaction between next nearest neighbors, third nearest neighbors, etc. (see, e.g., Ref. [5]). Two spin interactions do not always provide a sufficient representation of the interactions in a magnetic system. A more accurate description of the isotropic ferromagnet EuS for example also requires a three spin exchange interaction [6] of the type

$$\mathcal{H}_3 = -J_3 \sum_{\langle k,l,m \rangle} (\mathbf{S}_k \cdot \mathbf{S}_l) (\mathbf{S}_k \cdot \mathbf{S}_m), \quad (1.2)$$

where $\langle k, l, m \rangle$ denotes a triple of nearest neighbor spins. Four spin exchange coupling constants are often negligible, but the biquadratic interaction given by

$$\mathcal{H}_4 = -J_4 \sum_{\langle k,l \rangle} (\mathbf{S}_k \cdot \mathbf{S}_l)^2, \quad (1.3)$$

which is well known from the Blume - Emery - Griffith (BEG) model [7], needs to be considered in certain cases [8].

The thermodynamic properties of the model can be obtained from a Monte-Carlo simulation of the Hamiltonian $\mathcal{H}_{tot} = \mathcal{H} + \mathcal{H}_3 + \mathcal{H}_4$ given by Eqs.(1.1), (1.2), and (1.3). In order to study the *dynamic* properties of the spin system the equations of motion given by [1-4]

$$\frac{d}{dt} \mathbf{S}_k = \frac{\partial \mathcal{H}_{tot}}{\partial \mathbf{S}_k} \times \mathbf{S}_k \quad (1.4)$$

must be integrated numerically, where a Monte-Carlo simulation of the model provides *equilibrium* configurations as initial conditions for Eq.(1.4). Note that frequencies will be measured in energy units so that $\hbar = 1$ in Eq.(1.4). A typical quantity to be determined from the dynamics of the model is the dynamic structure factor $S(\mathbf{q}, \omega)$, which is given by the space-time Fourier transform of the spin-spin correlation function

$$\mathcal{G}^{\alpha, \beta}(\mathbf{r}_k - \mathbf{r}_l, t - t') \equiv \langle S_k^\alpha(t) S_l^\beta(t') \rangle, \quad (1.5)$$

where $\alpha, \beta = x, y, z$ denote the spin component, \mathbf{r}_k and \mathbf{r}_l are lattice vectors, and the average $\langle \dots \rangle$ must be taken over a sufficiently large number of independent initial *equilibrium* configurations. The effect of collective thermal excitations of the system (e.g., phonons) is not included in the above approach. However, in magnetic systems the typical time scale on which Eq.(1.4) has to be integrated is much shorter than typical time scales set by these excitations, so that the above procedure can be justified. In general one has to resort to the solution of Langevin equations rather than Eq.(1.4) in order to obtain the correct dynamics, but this is beyond the scope of this article.

From the above outline of a typical Monte-Carlo spin dynamics study it is evident, that at least in $d = 3$ the major part of the CPU time needed for a spin dynamics simulation is consumed by the numerical integration of Eq.(1.4). It is therefore desirable to do the integration with the biggest possible time step. However, using standard methods a severe restriction on the size of the time step is posed by the accuracy within which the numerical method observes the *conservation laws* of the dynamics. It is evident from Eq.(1.4) that $|\mathbf{S}_k|$ for each lattice site k and the total energy are conserved. Symmetries of the Hamiltonian impose additional conservation laws. If, for example, $\mathcal{H}_{tot} = \mathcal{H}$ according to Eq.(1.1) for $D = 0$ and $\lambda = 1$ (isotropic Heisenberg model) the magnetization $\mathbf{M} = \sum_k \mathbf{S}_k$ is a conserved quantity. For the anisotropic Heisenberg model, i.e., $\lambda \neq 1$ and/or $D \neq 0$ only the z -component M_z of the magnetization is conserved. Conservation of spin length and energy is particularly crucial, because the condition $|\mathbf{S}_k| = 1$ is a major part of the definition of the model and the energy of a configuration determines its statistical weight. It would therefore also be desirable to devise an algorithm which conserves these two quantities *exactly*.

The outline for the remainder of this investigation is as follows. In Sec.II we describe the properties of the currently used fourth-order predictor-corrector method [1-4]. Sec.III is devoted to the presentation of our new integration procedure, based on Trotter-Suzuki decompositions of exponential operators, which conserve spin length and, for the isotropic case only, energy *exactly*. In Sec.IV we compare both schemes with special regard to the accuracy within which the conservation laws hold and their speed for a given demand on accuracy. A comparison within the full framework of a spin dynamics simulation for a Heisenberg ferromagnet is also presented. We finally discuss the prospects of both algorithms in view of large scale spin dynamics simulations in Sec.V.

II. PREDICTOR-CORRECTOR METHODS

Predictor-corrector methods provide a very general tool for the numerical integration of initial value problems like Eq.(1.4) with an equilibrium configuration as the initial value. The demand for very good spin length and energy conservation, however, requires methods with small truncation errors in the time step δt . Further stability requirements for long times have led to the implementation of a fourth-order scheme, which we briefly reproduce here for the convenience of the reader.

In a more symbolic form Eq.(1.4) can be written as $\dot{y} = f(y)$ with the initial condition $y(0) = y_0$, where y is a short-hand notation of a complete spin configuration written, e.g., as a $3N$ dimensional vector for a lattice with N sites. The initial equilibrium configuration is simply denoted by y_0 . The predictor step of the scheme is then given, e.g., by the explicit Adams-Bashforth four-step method [9]

$$y(t + \delta t) = y(t) + \frac{\delta t}{24} [55f(y(t)) - 59f(y(t - \delta t)) + 37f(y(t - 2\delta t)) - 9f(y(t - 3\delta t))] \quad (2.1)$$

which has a local truncation error of the order $(\delta t)^5$. The corrector step consists of typically one iteration of the implicit Adams-Moulton three-step method [9]

$$y(t + \delta t) = y(t) + \frac{\delta t}{24} [9f(y(t + \delta t)) + 19f(y(t)) - 5f(y(t - \delta t)) + f(y(t - 2\delta t))] \quad (2.2)$$

which also has a local truncation error of the order $(\delta t)^5$. The first application of Eq.(2.1) obviously requires the knowledge of $y(\delta t)$, $y(2\delta t)$, and $y(3\delta t)$ apart from $y(0) = y_0$. These can be provided by three successive integrations of $\dot{y} = f(y)$ (see Eq.(1.4)) by the fourth-order Runge-Kutta method [9] which cannot be used for the entire time integration, because truncation errors accumulate too fast during typical integration times required for high frequency resolution. In order to apply Eqs.(2.1) and (2.2) repeatedly the spin configuration at the last four time steps must be kept in memory.

It is interesting to note that the predictor-corrector method according to Eqs.(2.1) and (2.2) observes the conservation laws for the magnetization according to the symmetry of the Hamiltonian to within machine accuracy if periodic boundary conditions are employed. The reason is that all spins are updated simultaneously by Eqs.(2.1) and Eq.(2.2) and that the driving forces (torques) are evaluated precisely according to the exact equation of motion (see Eq.(1.4)) for every time step. The periodic boundary conditions restore the discrete translational invariance of the infinite lattice in the finite sample needed for the simulation.

The predictor-corrector method is very general and, therefore, its implementation is independent of the special structure of the right-hand side of the equation of motion. Apart from the conservation of the magnetization the other conservation laws discussed in Sec.I will therefore only be observed within the accuracy set by the truncation error of the method. In practice, this limits the time step to typically $\delta t = 0.01/J$ in $d = 3$ [4] for the isotropic model Hamiltonian given by Eq.(1.1) ($D = 0$), where the total integration time is of the order $200/J$. The same method has also been used in $d = 2$ with a time step $\delta t = 0.025/J$ [2], but in this case the total integration time did not exceed $60/J$. In view of the fact that a time resolution of typically $0.1/J - 0.2/J$ is desired for the evaluation of the time displaced correlation function given by Eq.(1.5), it is clear that the total CPU time required for a spin dynamics simulation in $d = 3$ is dominated by the numerical integration of the equations of motion. A quantitative analysis is presented in Sec.IV.

III. SUZUKI-TROTTER DECOMPOSITION METHODS

The motion of a spin according to Eq.(1.4) may be visualized as a Larmor precession of the spin \mathbf{S} around an effective axis Ω which is itself time dependent. In order to illustrate our reasoning we restrict ourselves again to the Hamiltonian $\mathcal{H}_{tot} = \mathcal{H}$ given by Eq.(1.1) for the simple case $D = 0$ but for arbitrary values of λ . The evaluation of the right-hand side of Eq.(1.4) then shows that the lattice can be decomposed into two sublattices such that a spin on one sublattice performs a Larmor precession in a local field Ω of neighbor spins which are *all* located on the other sublattice. For the Hamiltonian given by Eq.(1.1) there are only two such sublattices if the underlying lattice is, e.g., simple cubic or bcc.

The first basic idea of the algorithm to be described below is to actually perform a *rotation* of a spin about its local field Ω by an angle $\alpha = |\Omega|\delta t$, rather than integrating Eq.(1.4) by some standard method. This procedure guarantees the conservation of the spin length $|\mathbf{S}|$ to within machine accuracy. (A procedure like this has already been implemented in a numerical study of spin motions in a classical ferromagnet [10]). The second basic idea is to exploit the sublattice decomposition of Eq.(1.4) to also ensure *energy* conservation to within machine accuracy. Denoting the two sublattices by \mathcal{A} and \mathcal{B} , respectively, we can write Eq.(1.4) in the form

$$\frac{d}{dt}\mathbf{S}_{k \in \mathcal{A}} = \Omega_{\mathcal{B}}[\{\mathbf{S}\}] \times \mathbf{S}_{k \in \mathcal{A}} \quad , \quad \frac{d}{dt}\mathbf{S}_{k \in \mathcal{B}} = \Omega_{\mathcal{A}}[\{\mathbf{S}\}] \times \mathbf{S}_{k \in \mathcal{B}}, \quad (3.1)$$

where $\Omega_{\mathcal{A}}[\{\mathbf{S}\}]$ and $\Omega_{\mathcal{B}}[\{\mathbf{S}\}]$ denote the local fields produced by the spins on sublattice \mathcal{A} and \mathcal{B} , respectively. Either of the equations in Eq.(3.1) reduces to a *linear* system of differential equations if the spins on the other sublattice are kept fixed. This suggests an *alternating* update scheme, i.e., the spins $\mathbf{S}_{k \in \mathcal{A}}$ are rotated for the given values of $\mathbf{S}_{k \in \mathcal{B}}$ and vice versa. This implies that the scalar products $\mathbf{S}_{k \in \mathcal{A}} \cdot \Omega_{\mathcal{B}}[\{\mathbf{S}\}]$ remain constant during the update of $\mathbf{S}_{k \in \mathcal{A}}$ and the scalar products $\mathbf{S}_{k \in \mathcal{B}} \cdot \Omega_{\mathcal{A}}[\{\mathbf{S}\}]$ remain constant during the update of $\mathbf{S}_{k \in \mathcal{B}}$. From Eq.(1.1) for $D = 0$ and Eq.(1.4) we therefore find that the energy is *exactly* conserved during this alternating update scheme (see also Eq.(3.4)). Note, that each sublattice rotation is performed with the *actual* values of the spins on the other sublattice, so that only a *single* copy of the spin configuration is kept in memory at any time. However, the magnetization will not be conserved during the above rotation operations. Moreover, the two alternating rotation operations do not commute, so that a closer examination of the sublattice decomposition of the spin rotation is required.

In order to obtain a simple description of the operations performed on the spin configuration during the integration of the equations of motion we again represent a full configuration by a vector y which is decomposed into two sublattice components $y_{\mathcal{A}}$ and $y_{\mathcal{B}}$ according to $y = (y_{\mathcal{A}}, y_{\mathcal{B}})$. The cross products in Eq.(3.1) can be expressed by matrices A and B which are the infinitesimal generators of the rotation of the spin configuration $y_{\mathcal{A}}$ on sublattice \mathcal{A} at fixed $y_{\mathcal{B}}$ and of the spin configuration $y_{\mathcal{B}}$ on sublattice \mathcal{B} at fixed $y_{\mathcal{A}}$, respectively. The exact update of the configuration y from time t to $t + \delta t$ can then be expressed by an exponential (matrix) operator according to

$$y(t + \delta t) = e^{(A+B)\delta t} y(t). \quad (3.2)$$

Although the exponential operator in Eq.(3.2) rotates each spin of the configuration it has no simple explicit form, because the rotation axis for each spin depends on the configuration itself (see Eq.(3.1)) and is therefore not known *a priori*. However, the operators $e^{A\delta t}$ and $e^{B\delta t}$ which rotate $y_{\mathcal{A}}$ at fixed $y_{\mathcal{B}}$ and $y_{\mathcal{B}}$ at fixed $y_{\mathcal{A}}$, respectively, *do* have a simple explicit form. We demonstrate this for the case $\lambda = 1$ and $D = 0$ in Eq.(1.1). For each $k \in \mathcal{A}$ we find

$$\Omega_{\mathcal{A}}[\{\mathbf{S}\}] = -J \sum_{l=NN(k)} \mathbf{S}_l \equiv \Omega_k, \quad (3.3)$$

where $NN(k)$ denotes the nearest neighbors of k (which belong to $y_{\mathcal{B}}$). Eq.(3.3) can be readily generalized for $\lambda \neq 1$, the case $D \neq 0$ will be discussed below. From Eqs.(3.1) and (3.3) we obtain (see also Ref. [10])

$$\mathbf{S}_k(t + \delta t) = \frac{\Omega_k(\Omega_k \cdot \mathbf{S}_k(t))}{\Omega_k^2} + \left[\mathbf{S}_k(t) - \frac{\Omega_k(\Omega_k \cdot \mathbf{S}_k(t))}{\Omega_k^2} \right] \cos(|\Omega_k|\delta t) + \frac{\Omega_k \times \mathbf{S}_k(t)}{|\Omega_k|} \sin(|\Omega_k|\delta t). \quad (3.4)$$

Note, that according to Eq.(3.4) $\Omega_k \cdot \mathbf{S}_k(t + \delta t) = \Omega_k \cdot \mathbf{S}_k(t)$ which explicitly confirms energy conservation. For $k \in \mathcal{B}$ Eq.(3.4) also holds in exactly the same form. The alternating update scheme for the integration of Eq.(3.1), i.e., Eq.(1.4) now amounts to the replacement $e^{(A+B)\delta t} \rightarrow e^{A\delta t} e^{B\delta t}$ in Eq.(3.2), which is only correct up to terms of the order $(\delta t)^2$ [11]. The magnetization will therefore only be conserved up to terms of the order δt (global truncation error), which is insufficient for practical purposes. The remedy for this shortcoming, which constitutes the third basic idea of the algorithm, is now obvious. We simply employ higher order Suzuki-Trotter decompositions of the exponential operator in Eq.(3.2) to increase the order of the local truncation error of the algorithm and thus improve the magnetization conservation. The simplest possible improvement is given by the well known second order decomposition [11]

$$e^{(A+B)\delta t} = e^{A\delta t/2} e^{B\delta t} e^{A\delta t/2} + \mathcal{O}(\delta t^3), \quad (3.5)$$

which will be used for comparison with the predictor-corrector method outlined in Sec.II. Note, that Eq.(3.5) is equivalent to the midpoint integration method applied to Eq.(3.1) (see also Ref. [10]). We furthermore use the fourth order decomposition [11]

$$e^{(A+B)\delta t} = \prod_{i=1}^5 e^{p_i A\delta t/2} e^{p_i B\delta t} e^{p_i A\delta t/2} + \mathcal{O}(\delta t^5) \quad (3.6)$$

with the parameters

$$p_1 = p_2 = p_4 = p_5 \equiv p = 1/(4 - 4^{1/3}) \quad \text{and} \quad p_3 = 1 - 4p. \quad (3.7)$$

It is also possible to construct a decomposition like Eq.(3.6) with only three factors, but then $|p_i| > 1$ for $i = 1, 2, 3$ which is numerically unfavorable [11]. From Eqs.(3.5) and (3.6) the close analogy to symplectic integrators obtained from the Liouville operator formalism for Molecular Dynamics simulations is obvious [12]. The sublattice decomposition of the spin degrees of freedom in spin dynamics corresponds to the natural decomposition of the degrees of freedom in Hamiltonian dynamics into positions and momenta. Especially the second order decomposition given by Eq.(3.5) is equivalent to the velocity Verlet algorithm for Molecular Dynamics simulations [13] (see also Ref. [12] for recent developments in this field) which itself is equivalent to the well-known leapfrog algorithm [12].

As will be shown in Sec.IV, the additional computational effort to be invested in the evaluation of Eq.(3.6) as compared to Eq.(3.5) or Eqs.(2.1) and (2.2) can be compensated by using larger time steps. The evaluation of the trigonometric functions in Eq.(3.4) can also be avoided by observing that the above decompositions are only correct to within a certain order in δt . It is therefore sufficient to replace $\sin x$ by its Taylor polynomial $T(x)$, where $T(x) = x$ if Eq.(3.5) is used and $T(x) = x - x^3/6$ if Eq.(3.6) is used. The cosine in Eq.(3.4) then has to be replaced by $\sqrt{1 - T^2(x)}$

in order to maintain conservation of spin length. It is also worth noting that the above decompositions maintain the time inversion property of $e^{(A+B)\delta t}$, i.e., their inverse is obtained by the replacement $\delta t \rightarrow -\delta t$. A Hamiltonian with both nearest and next-nearest neighbor two-spin interactions on, e.g., simple cubic or bcc lattices, can be treated within the above framework if the lattice is decomposed into four sublattices. In contrast to the predictor - corrector method conservation of magnetization according to the symmetry of the Hamiltonian is only observed within the truncation error of the decomposition method, because according to Eqs.(3.5) and (3.6) the sublattices \mathcal{A} and \mathcal{B} are no longer strictly equivalent.

We now generalize the above considerations to the case $D \neq 0$ in Eq.(1.1). For a spin in sublattice \mathcal{A} the equation of motion reads

$$\frac{d}{dt}\mathbf{S}_{k \in \mathcal{A}} = \Omega_{\mathcal{B}}[\{\mathbf{S}\}] \times \mathbf{S}_{k \in \mathcal{A}} - 2DS_{k \in \mathcal{A}}^z \mathbf{e}_z \times \mathbf{S}_{k \in \mathcal{A}}, \quad (3.8)$$

where \mathbf{e}_z denotes the unit vector pointing along the z -axis, and spins in sublattice \mathcal{B} obey an equation of the same form. In contrast to the isotropic case (see Eq.(3.1)) the equation of motion for each individual spin on each sublattice is *nonlinear*. It is possible to obtain an analytic solution of this equation, in the spirit of Eq.(3.4), where the trigonometric functions are basically replaced by Jacobian elliptic functions, and to implement this solution as a rotation operation in one of the above decomposition schemes. This approach, however, involves very precision sensitive operations which greatly limit speed and therefore the overall efficiency of such an algorithm. In practice, it is much more convenient to include the effects of the nonlinearity in Eq.(3.8) by an iterative method, as described in the following paragraph.

For the sublattice decomposition of the spin rotation in the isotropic case discussed above the requirement for energy conservation in the presence of a single site anisotropy reads

$$\Omega_k \cdot \mathbf{S}_k(t + \delta t) - D [S_k^z(t + \delta t)]^2 = \Omega_k \cdot \mathbf{S}_k(t) - D [S_k^z(t)]^2 \quad (3.9)$$

for $k \in \mathcal{A}$ and $k \in \mathcal{B}$, where Ω_k is given by Eq.(3.3). In order to perform a rotation operation in analogy to Eq.(3.4) we have to identify an effective rotation axis. This can be achieved by rewriting Eq.(3.9) in the form $\tilde{\Omega}_k \cdot (\mathbf{S}_k(t + \delta t) - \mathbf{S}_k(t)) = 0$, where $\tilde{\Omega}_k$ is given by

$$\tilde{\Omega}_k = \Omega_k - D(0, 0, S_k^z(t) + S_k^z(t + \delta t)), \quad (3.10)$$

i.e., in order to perform the rotation S_k^z at the future time $t + \delta t$ must be known in *advance*. This problem can only be solved iteratively starting from the initial value $S_k^z(t + \delta t) = S_k^z(t)$ in Eq.(3.10) and performing several updates according to the decompositions given by Eqs.(3.5) or (3.6), respectively, in order to improve energy conservation according to Eq.(3.9). Naturally, this procedure leads to a substantial slowdown of the integration algorithm, where the energy is no longer exactly conserved. Details are discussed in Sec.IV. The biquadratic interaction given by Eq.(1.3) can be treated by the same iterative scheme. The three-spin interaction given by Eq.(1.2), however, requires a reconsideration of the sublattice decomposition. Specific numerical examples in comparison with those obtained from the predictor-corrector method are presented in the following section.

IV. THE METHODS IN COMPARISON

For a quantitative analysis of the integration methods outlined above we restrict ourselves to the Hamiltonian $\mathcal{H}_{tot} = \mathcal{H}$ given by Eq.(1.1) for $\lambda = 1$ in $d = 3$. The underlying lattice is simple cubic with $L = 10$ lattice sites in each direction and periodic boundary conditions are imposed in all cases discussed below. The simulations have been performed on IBM RS/6000 workstations at the Center for Simulation Physics and a Cray C90 at the Pittsburgh Supercomputer Center.

In order to compare the different integration methods we first investigate the accuracy within which the conservation laws are fulfilled. As a standard initial configuration we choose a well equilibrated configuration from a Monte-Carlo simulation of the model defined by Eq.(1.1) for $\lambda = 1$ at a temperature $T = 0.8T_c$ for $D = 0$ and $D = J$, where T_c refers to the critical temperature of the isotropic model ($D = 0$) and is given by $K_c = J/(k_B T_c) = 0.693035$ [14]. The magnetization of such a configuration differs from zero and provides an indicator for the numerical quality of the magnetization conservation. We integrate the equations of motion to $t = 800/J$ and monitor the energy $e(t) \equiv E(t)/(JL^3)$ of the configuration per spin and in units of the exchange coupling constant J and the modulus $m(t) \equiv |\mathbf{M}(t)|/L^3$ of the magnetization per spin for the isotropic case $D = 0$ and its z -component $m_z(t) \equiv M_z(t)/L^3$ for the strongly anisotropic case $D = J$ as functions of time. Note, that for these tests both integration methods are started from identical initial configurations. The time step for the predictor-corrector method is chosen as $\delta t = 0.01/J$ in all cases.

We first consider the case of $D = 0$ for which the implementation of Eqs.(3.5) and (3.6) using Eq.(3.4) is straightforward. The Taylor polynomial $T(x)$ is chosen as $T(x) = x - x^3/6$ for Eq.(3.5) and $T(x) = x - x^3/6 + x^5/120$ for Eq.(3.6) in order to reduce the amplitude of the magnetization fluctuations. Fig.1 shows that $e(t)$ for the predictor-corrector method increases linearly with time whereas the decomposition methods both yield a constant value for $e(t)$ as shown in Fig.1. Fig.2 displays the magnetization conservation for the predictor-corrector method ($\delta t = 0.01/J$) and the second order decomposition method according to Eq.(3.5) for $\delta t = 0.04/J$. The predictor-corrector method conserves $m(t)$ *exactly*, whereas the second order decomposition causes fluctuations of $m(t)$ on all time scales. The apparent deviation of the temporal average of the magnetization from the exact value is due to the finite sample time; for times greater than $2000/J$ the deviation changes sign and fluctuations on time scales larger than $800/J$ become visible. The temporal structure of $m(t)$ for the decomposition methods given by Eq.(3.5) for $\delta t = 0.04/J$ and Eq.(3.6) for $\delta t = 0.2/J$ is displayed in Fig.3. It is remarkable that the fourth order decomposition gives a substantially better magnetization conservation than the second order decomposition despite the very large time step. In order to achieve the same overall accuracy of the magnetization conservation with the second order decomposition a time step $\delta t < 0.02/J$ is necessary. A single integration of the equations of motion using Eq.(3.5) (second order decomposition) is about twice as fast as the predictor-corrector method used here. The more complex fourth order decomposition (see Eq.(3.6)), however, is about 2.5 times slower than the predictor corrector method. Taking the increase in time step by factors of 4 and 20, respectively, into account, we find that both decomposition methods yield an eightfold speedup of the integration of the equation of motion. If the overall quality of the magnetization conservation is also taken into account, there is a clear advantage for the fourth order decomposition according to Eq.(3.6) for the isotropic case $D = 0$.

We now turn to the strongly anisotropic case $D = J$. The predictor-corrector method can be applied as before, but the decomposition scheme needs a major modification because the spin rotation axis depends on the spin value S_k^z at the future time $t + \delta t$ (see Eq.(3.10)). As already pointed out in Sec.III this gives rise to a self consistency problem which can be solved iteratively, where the quality of the energy conservation depends on the number of iterations performed. For the second order decomposition (see Eq.(3.5)) and the time step $\delta t = 0.04/J$ two iterations are sufficient to obtain a better energy conservation than the predictor-corrector method. This means that a single integration of the equations of motion using the second order decomposition takes twice as long as for $D = 0$, so that its advantage in speed only comes from the increase in the time step, which is still a factor of four. For the fourth order decomposition according to Eq.(3.6) with $\delta t = 0.2/J$ six iterations are needed to obtain energy conservation to within six significant digits, which makes one integration with the fourth order decomposition 15 times slower than one integration with the predictor-corrector method. From the increase of δt by a factor 20 only a 30% gain in speed remains for Eq.(3.6). The number of iterations needed decreases with δt , but this decrease does not compensate the loss in speed due to the smaller time step. However, one still obtains a greatly improved energy conservation. The direct comparison of the energy conservation is shown in Fig.4. All three methods behave in a similar way, the change in energy is basically linear with time. The reason for this is the iterative nature of all three methods in the case $D \neq 0$. The magnetization fluctuations shown in Fig.5 for the predictor-corrector and the second order decomposition method ($\delta t = 0.04/J$) reveal the same behavior of both methods as shown in Fig.2 for $D = 0$. The direct comparison between the second and fourth order decomposition for $\delta t = 0.04/J$ and $\delta t = 0.2/J$, respectively, is displayed in Fig.6. The overall accuracy of the magnetization conservation appears to be independent of D for both decomposition methods. If the emphasis is put on overall energy conservation *and* speed, the second order decomposition given by Eq.(3.5) has some advantages over the predictor-corrector method. If the emphasis is put on energy conservation alone, the fourth order decomposition given by Eq.(3.6) shows the best performance, but it is only slightly faster than the predictor-corrector method.

We close this section with a direct comparison of the longitudinal ($S_l(\mathbf{q}, \omega)$) and transverse ($S_t(\mathbf{q}, \omega)$) components of the dynamic structure factor for the isotropic Heisenberg ferromagnet (see Eq.(1.1) for $D = 0$) on a simple cubic lattice ($L = 10$, periodic boundary conditions) at the temperature $T = 0.8T_c$ in the (100) direction. In order to measure $S_l(\mathbf{q}, \omega)$ one has to consider the projections of all spins onto the direction of the magnetization \mathbf{M} of the initial configuration. Note that in general \mathbf{M} for a given initial (equilibrium) spin configuration will be nonzero even in a finite system. Only the *average* $\langle \mathbf{M} \rangle$ of the magnetization over sufficiently many equilibrium configurations yields $\langle \mathbf{M} \rangle = 0$ within the statistical errors. The spin components transverse to \mathbf{M} then give access to $S_t(\mathbf{q}, \omega)$. The results are shown in Figs.7 and 8 for $\mathbf{q} = (\pi/5, 0, 0)$, where $S_l(\mathbf{q}, \omega)$ and $S_t(\mathbf{q}, \omega)$ have been normalized to the static structure factor $S_{l,t}(\mathbf{q}) \equiv \int_0^\infty S_{l,t}(\mathbf{q}, \omega) d\omega$. The diamonds represent the result for the predictor-corrector method ($\delta t = 0.01/J$) and the triangles show the result for the second order decomposition method (see Eq.(3.5), $\delta t = 0.04/J$). For both methods the equations of motion have been integrated to $800/J$ and averages have been taken over 1000 initial configurations, where the time displaced correlation functions have been measured to $400/J$. The statistical error indicated by the error bar represents one standard deviation. For the longitudinal structure factor shown in Fig.7 the statistical error is smaller than the symbol size. The overall agreement of the data is very good. The main maximum corresponds to the spin wave peak and is located at $\omega_0 = 0.25J$ in all cases. The frequency resolution is

$\delta\omega = 2\pi J/400 \simeq 0.016J$. The shoulder like feature at $\omega \simeq 0.5J$ in $S_l(\mathbf{q}, \omega)$ (see Fig.7) is due to many-spin wave processes, the description of which is beyond the scope of this article. Both methods have spent about the same CPU time on generating the initial configurations, but with the time steps given above, the integration of the equations of motion with the second order decomposition method is about eight times faster than with the predictor-corrector method. The discrepancy between the errorbars shown in Fig.8 is of statistical origin and indicates the statistical uncertainty of the errorbars themselves. Note, however, that the discrepancy only occurs in a frequency region well outside the spin wave peak, where the signal level is almost three orders of magnitude below its peak value.

V. SUMMARY

Starting from a well developed and established predictor-corrector method for the numerical integration of the equations of motion of a classical spin system as a timing and precision standard we devised and tested an alternative class of algorithms which is based on Suzuki-Trotter decompositions of exponential operators. Our findings can be summarized as follows.

1. Advantages of the predictor-corrector method

The greatest advantage of the predictor-corrector method is its versatility and its capability to conserve the magnetization exactly. Isotropic and anisotropic spins systems with nearest and next-nearest neighbor interactions can be treated within one and the same numerical approach. The decomposition of the lattice into sublattices, which is the basis for the decomposition method, depends on the range of the interactions, so that this numerical approach is far less general than the predictor-corrector method. Crystal field anisotropies leave the performance of the predictor-corrector method almost unaffected, whereas the decomposition method suffers from a drastic reduction in speed.

2. Advantages of the decomposition method

The greatest advantage of the decomposition method is its capability for handling large time steps and the exact conservation of spin length. In the absence of anisotropies it also conserves the energy exactly and it maintains reversibility. For anisotropic Hamiltonians energy conservation and reversibility can be obtained to a high accuracy using iterative schemes; exact magnetization conservation, however, is lost. The time steps typically used are unaccessible by the predictor-corrector method due to the lack of exact energy conservation within the algorithm. The resulting speedup of a spin dynamics simulation gives access to larger lattices, provided a second order decomposition is sufficiently accurate for the problem under investigation. In simple cases the fourth order decomposition yields very accurate results even for time steps an order of magnitude larger than typical time steps used for the predictor-corrector method.

A general recommendation for one or the other method cannot be given. If, however, special interactions are the main objective of the investigation, one should resort to the predictor-corrector method because of its generality. If the interactions in the system are standard two-spin exchange interactions and the objective is to study large systems, one should consider the decomposition method because of its speed and its built-in energy and spin length conservation.

ACKNOWLEDGMENTS

M. Krech gratefully acknowledges financial support of this work through the Heisenberg program of the Deutsche Forschungsgemeinschaft. This research was supported in part by NSF grant #DMR - 9405018 and the Pittsburgh Supercomputer Center.

Note added in proof

While this work was in press we have learned that a method equivalent to the one presented here had been developed independently by Frank, Huang, and Leimkuhler (J. Frank, W. Huang, and B. Leimkuhler, *Journal of Computational Physics* **133**, 160 (1997).) Frank, Huang, and Leimkuhler denote their method as *Staggered Red-Black Method* and employ the same decomposition technique which is described in this work.

- [1] H.G. Evertz and D.P. Landau, Phys. Rev. B **54**, 12302 (1996).
- [2] B.V. Costa, J.E.R. Costa, and D.P. Landau, J. Appl. Phys. **81**, 5746 (1997).
- [3] K. Chen and D.P. Landau, Phys. Rev. B **49**, 3266 (1994).
- [4] A. Bunker, K. Chen, and D.P. Landau, Phys. Rev. B **54**, 9259 (1996).
- [5] H.G. Bohm, W. Zinn, B. Dorner, and A. Kollmar, Phys. Rev. B **22**, 5447 (1980).
- [6] E. Mueller-Hartmann, U. Koebler, L. Smardz, J. Mag. Mag. Mat. **173**, 133 (1997)
- [7] M. Blume, V.J. Emery, and R.B. Griffith, Phys. Rev. A **4**, 1071 (1971).
- [8] O. N. Mryasov, A. J. Freeman, and A. I. Liechtenstein, J. Appl. Phys. **79**, 4805 (1996).
- [9] R.L. Burden, J.D. Faires, and A.C. Reynolds, *Numerical Analysis* (Prindle, Weber & Schmidt, Boston, 1981), p.205 and pp.219.
- [10] R.E. Watson, M. Blume, and G.H. Vineyard, Phys. Rev. **181**, 811 (1969).
- [11] H. Yoshida, Phys. Lett. A **150**, 262 (1990); see also M. Suzuki and K. Umeno in *Computer Simulation Studies in Condensed Matter Physics VI*, edited by D.P. Landau, K.K. Mon, and H.B. Schüttler (Springer, Berlin, 1993), pp. 74 and references therein.
- [12] A. Kopf, W. Paul, and B. Dünweg, Comp. Phys. Comm. **101**, 1 (1997) and references therein.
- [13] L. Verlet, Phys. Rev. **159**, 98 (1967).
- [14] K. Chen, A. M. Ferrenberg, and D. P. Landau, Phys. Rev. B **48**, 3249 (1993).

FIG. 1. Energy $e(t) = E(t)/(JL^3)$ per spin for the predictor-corrector method (see Eqs.(2.1) and (2.2)) for the time step $\delta t = 0.01/J$ and $D = 0$ (solid line). Both decomposition schemes (see Eqs.(3.5) and (3.6)) conserve the energy exactly (dashed line).

FIG. 2. Magnetization $m(t) = |\mathbf{M}(t)|/L^3$ per spin for the predictor-corrector method (see Eqs.(2.1) and (2.2)) for the time step $\delta t = 0.01/J$ (dashed line) and the second order decomposition scheme (see Eq.(3.5)) for the time step $\delta t = 0.04/J$ (solid line) for $D = 0$. The predictor-corrector method conserves the magnetization exactly, whereas Eq.(3.5) yields fluctuations in $m(t)$ on all time scales.

FIG. 3. Magnetization $m(t)$ per spin for the fourth order decomposition method (see Eq.(3.6)) with $\delta t = 0.2/J$ (solid line) and for the second order decomposition method (see Eq.(3.5)) with $\delta t = 0.04/J$ (dashed line) for $D = 0$. The CPU time needed for both methods with these time steps is almost the same. Despite the large time step the fourth order decomposition method yields substantially smaller magnetization fluctuations than the second order decomposition.

FIG. 4. Energy $e(t)$ per spin for the predictor-corrector method (see Eqs.(2.1) and (2.2)) for the time step $\delta t = 0.01/J$ and $D = J$ (solid line). The decomposition scheme given by Eq.(3.5) for $\delta t = 0.04/J$ shows a decrease of $e(t)$ (dashed line) and Eq.(3.6) for $\delta t = 0.2/J$ also yields a decrease of $e(t)$ (dotted line). For these parameters the decomposition methods show better energy conservation than the predictor-corrector method.

FIG. 5. Magnetization $m_z(t)$ per spin for the predictor-corrector method (see Eqs.(2.1) and (2.2)) for the time step $\delta t = 0.01/J$ (dashed line) and the second order decomposition scheme (see Eq.(3.5)) for the time step $\delta t = 0.04/J$ (solid line) and $D = J$. The qualitative behavior of $m_z(t)$ closely resembles the behavior in the isotropic case shown in Fig.2.

FIG. 6. Magnetization $m_z(t)$ per spin for the fourth order decomposition method (see Eq.(3.6)) with $\delta t = 0.2/J$ (solid line) and for the second order decomposition method (see Eq.(3.5)) with $\delta t = 0.04/J$ (dashed line) for $D = J$. The typical temporal structure of the fluctuations of $m_z(t)$ is very similar to the isotropic case shown in Fig.3.

FIG. 7. Longitudinal dynamic structure factor $S_l(\mathbf{q}, \omega)$ of an isotropic Heisenberg ferromagnet for $T = 0.8T_c$ and $|\mathbf{q}| = \pi/5$ in the (100) direction on a simple cubic lattice ($L = 10$, periodic boundary conditions) normalized to the static structure factor $S_l(\mathbf{q}) \equiv \int_0^\infty S_l(\mathbf{q}, \omega) d\omega$ for the predictor-corrector method (diamonds) and the second order decomposition method (triangles) for time steps $\delta t = 0.01/J$ and $\delta t = 0.04/J$, respectively (see main text). The statistical error (one standard deviation) is smaller than the symbol size.

FIG. 8. Transverse dynamic structure factor $S_t(\mathbf{q}, \omega)$ of an isotropic Heisenberg ferromagnet for $T = 0.8T_c$ and $|\mathbf{q}| = \pi/5$ in the (100) direction on a simple cubic lattice ($L = 10$, periodic boundary conditions) normalized to the static structure factor $S_t(\mathbf{q}) \equiv \int_0^\infty S_t(\mathbf{q}, \omega) d\omega$ for the predictor-corrector method (diamonds) and the second order decomposition method (triangles) for time steps $\delta t = 0.01/J$ and $\delta t = 0.04/J$, respectively (see main text). The error bars represent one standard deviation.

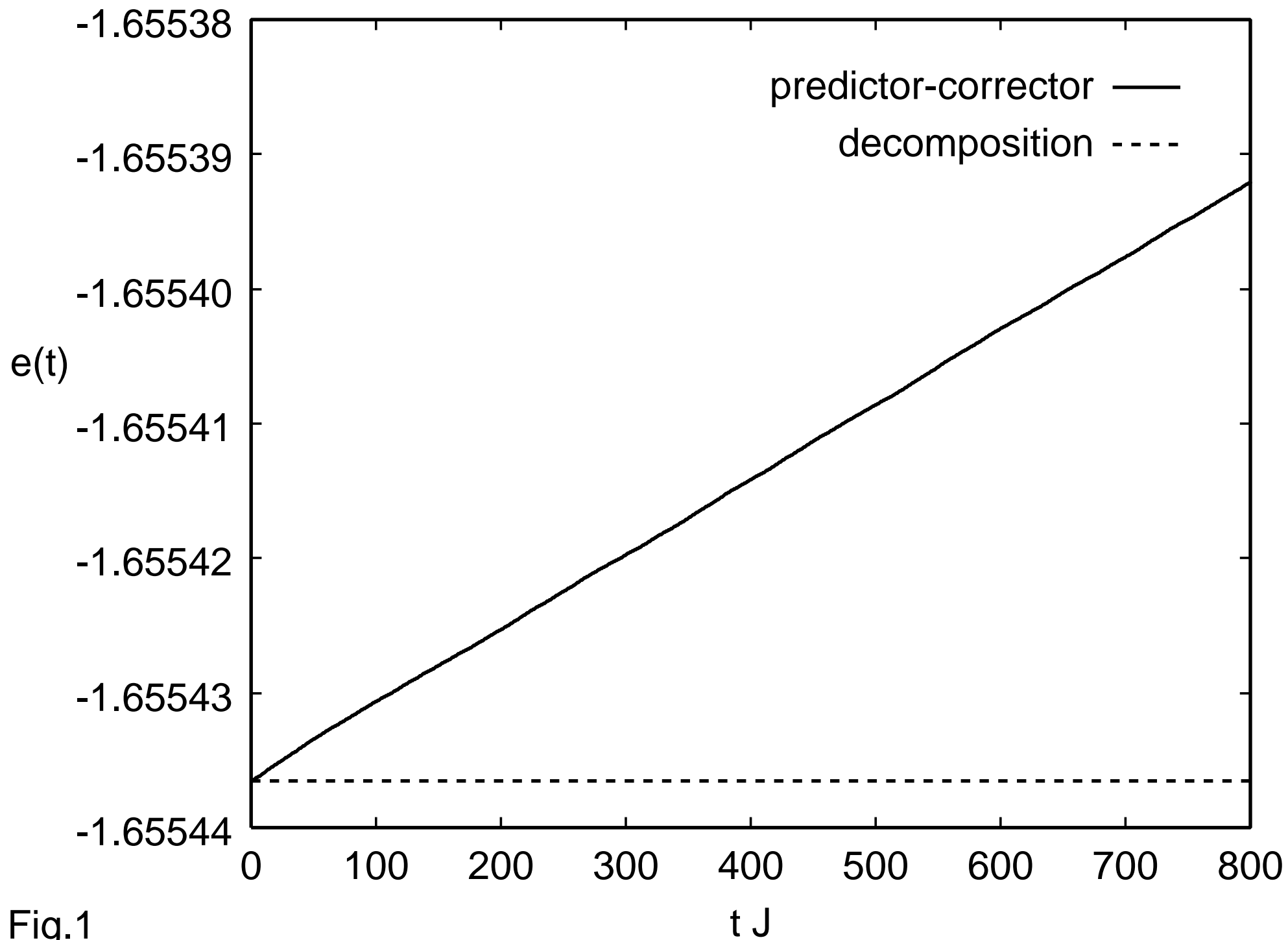


Fig.1

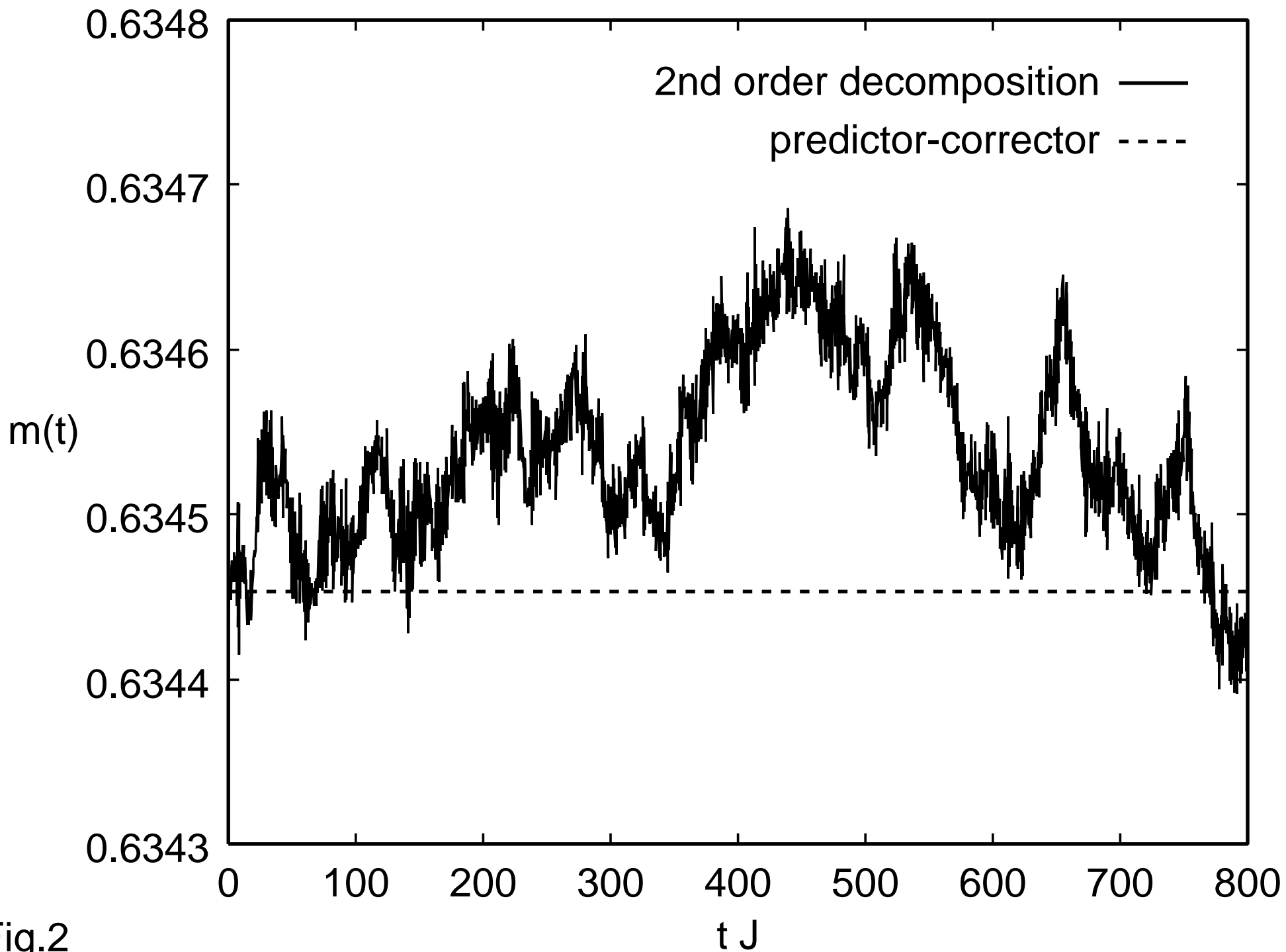


Fig.2

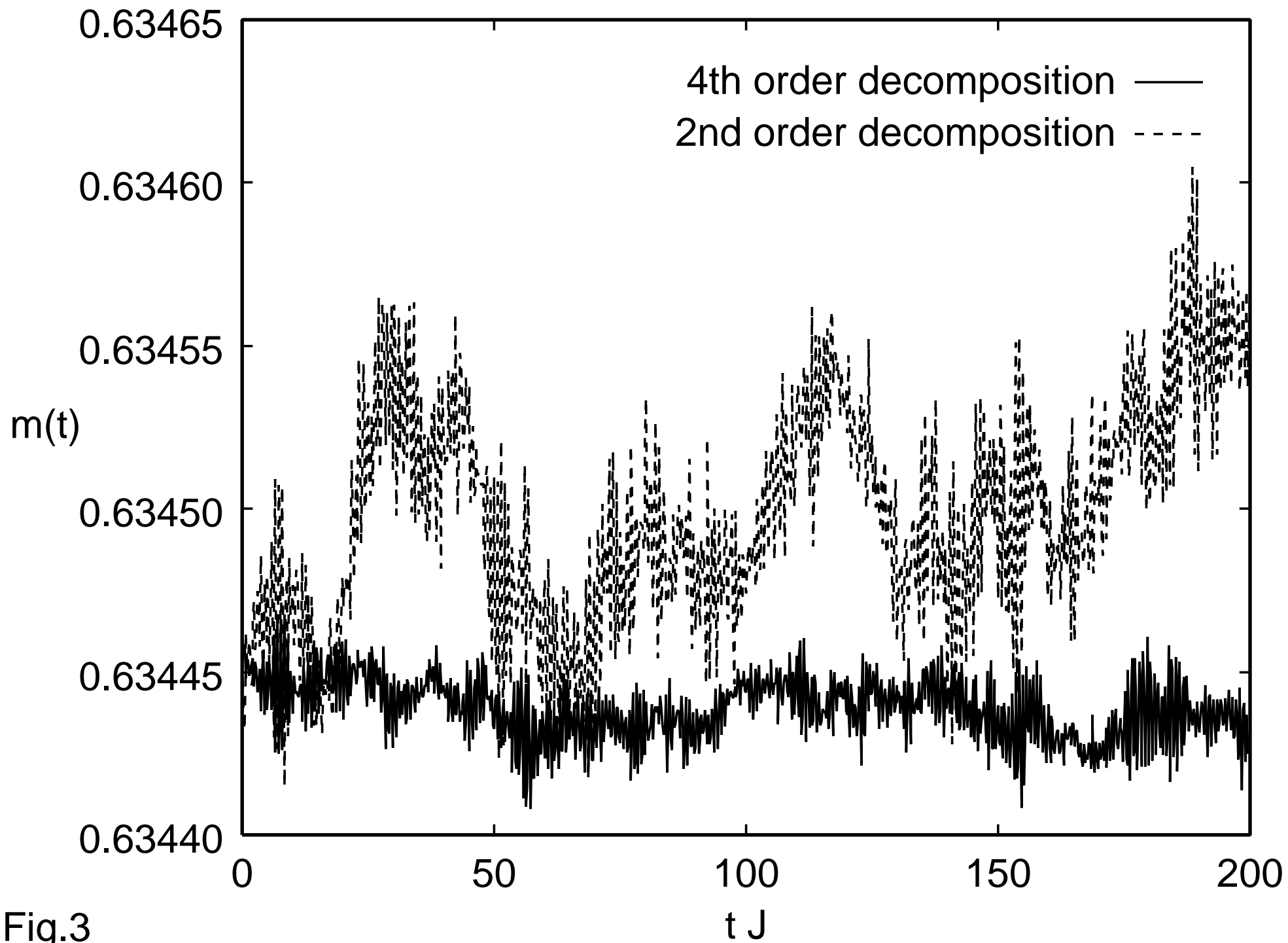


Fig.3

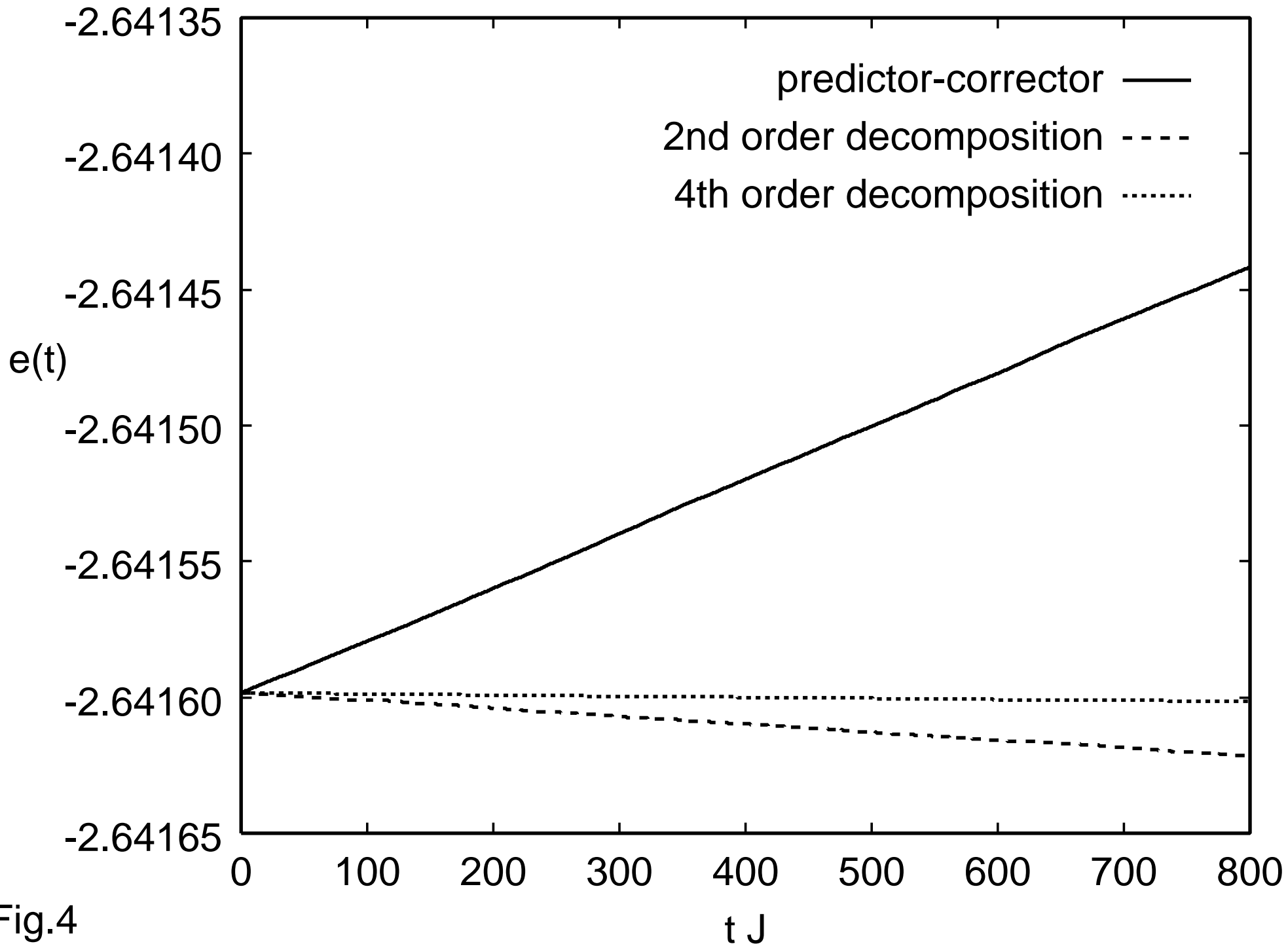


Fig.4

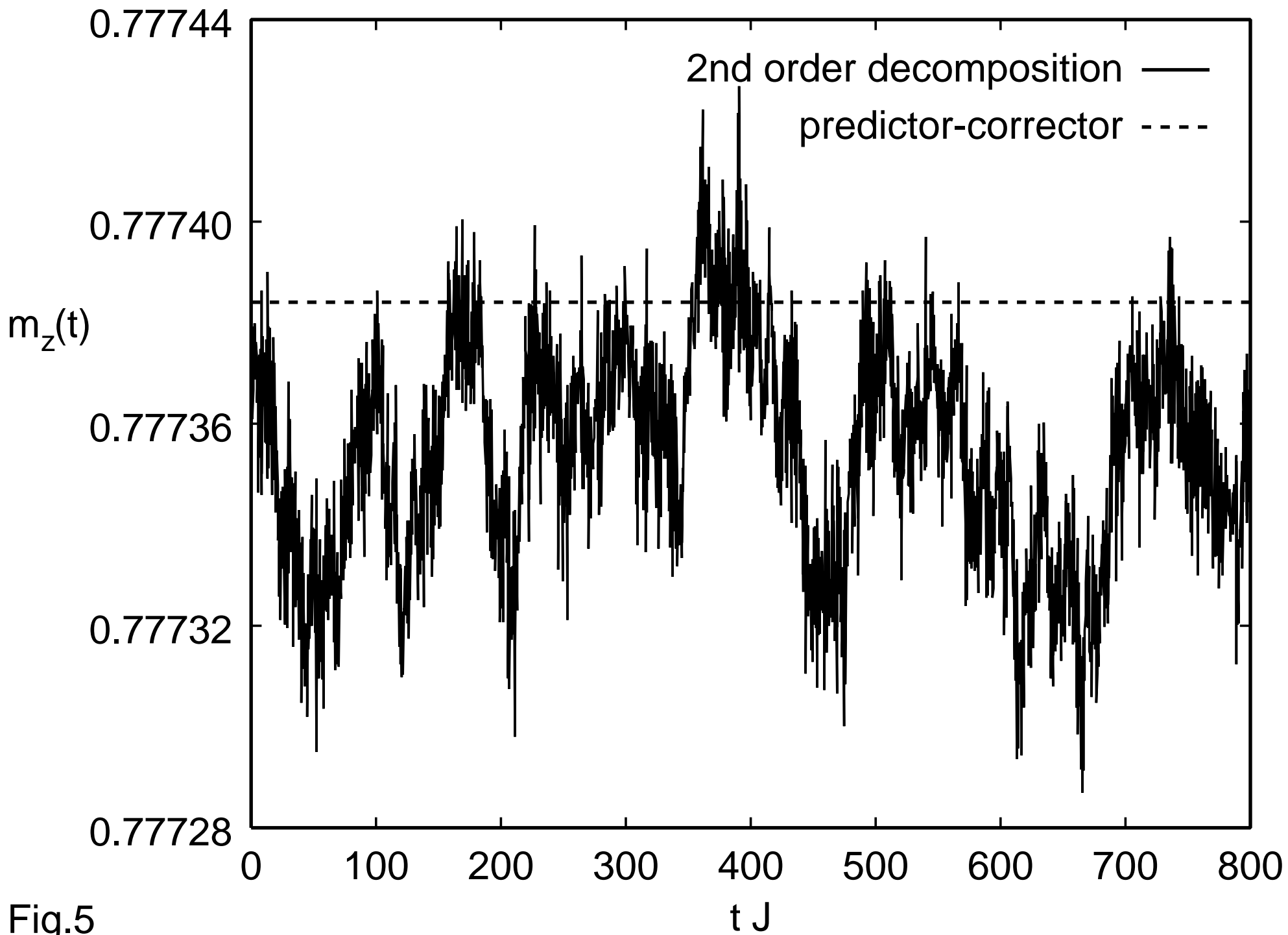


Fig.5

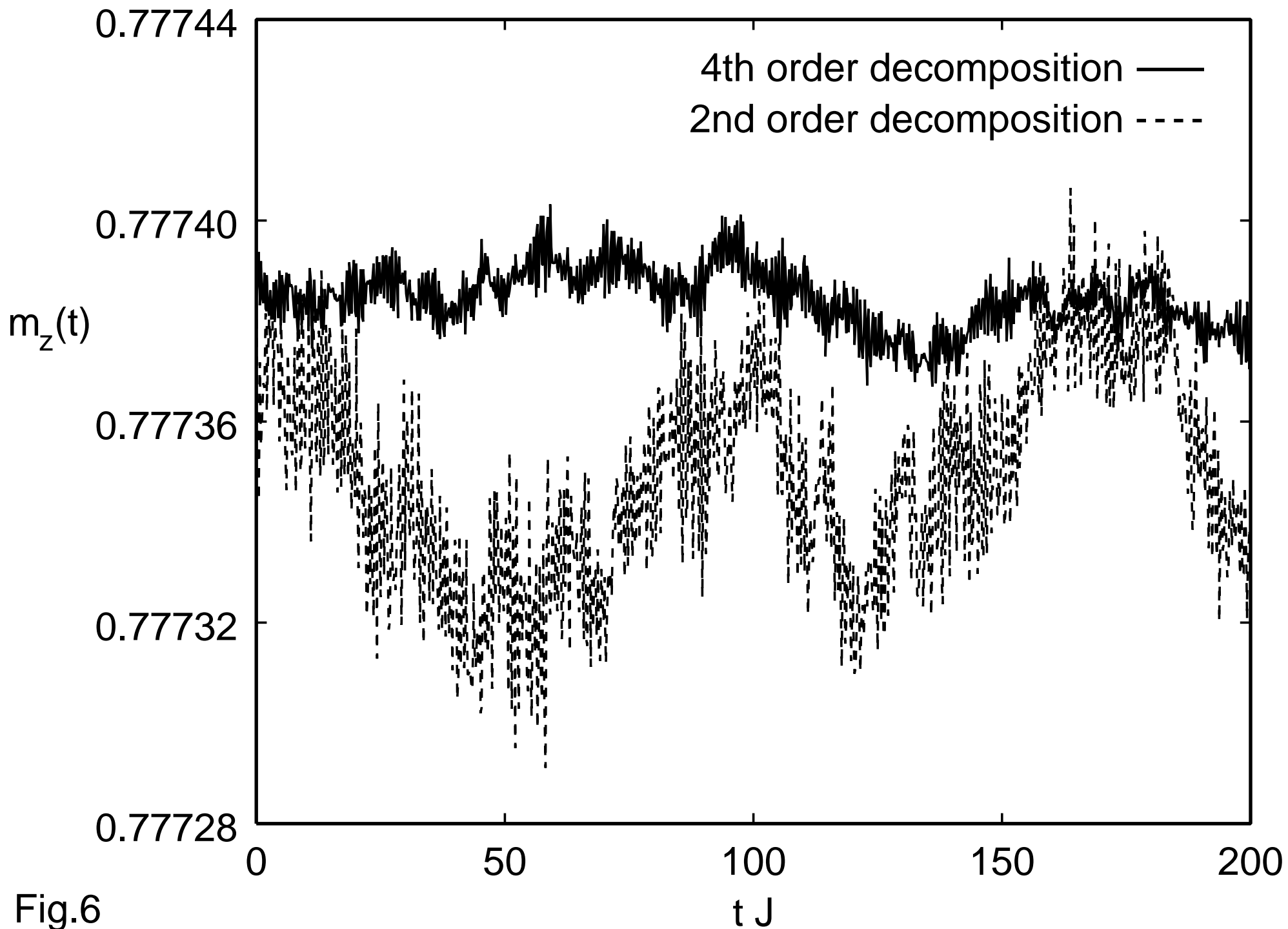


Fig.6

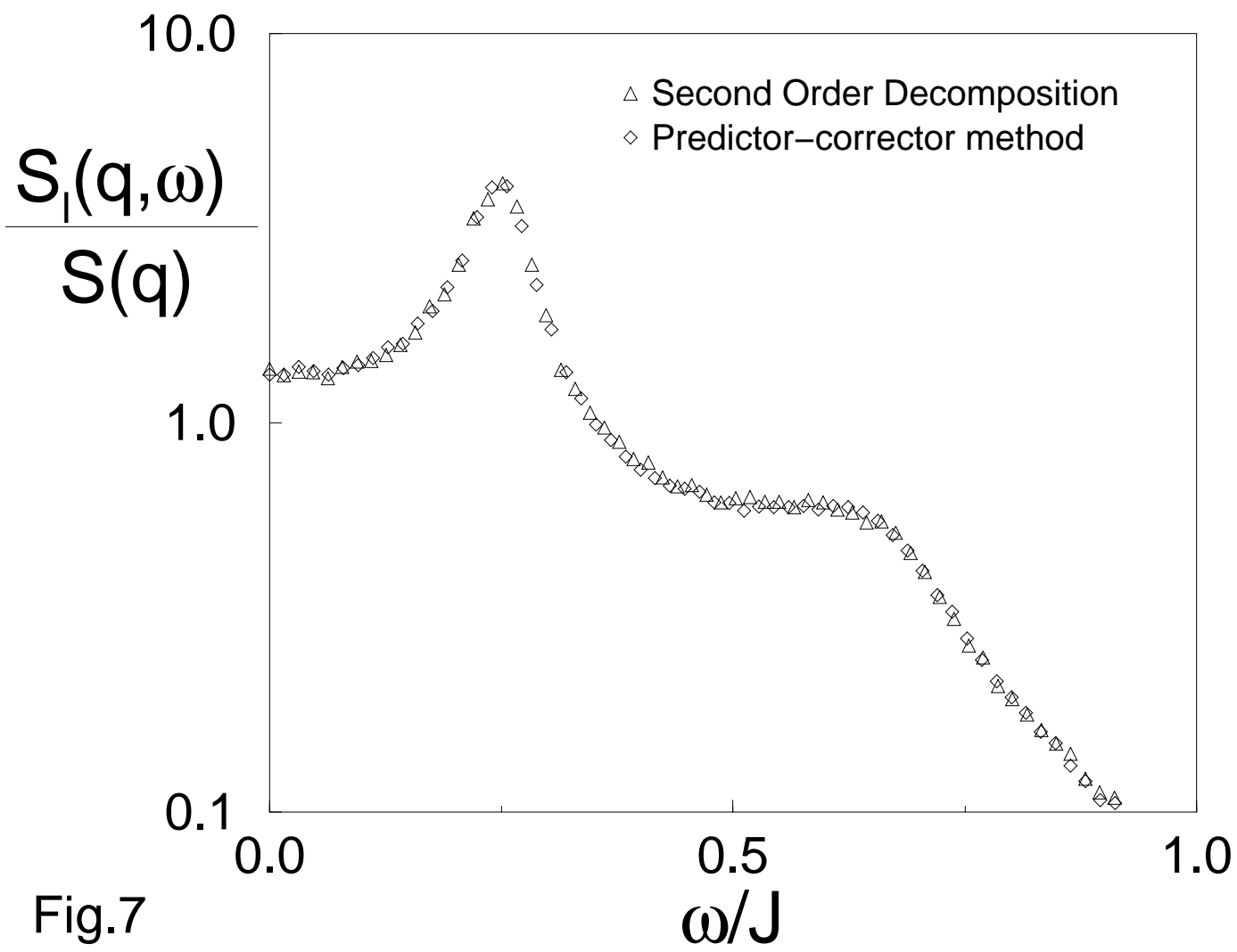


Fig.7

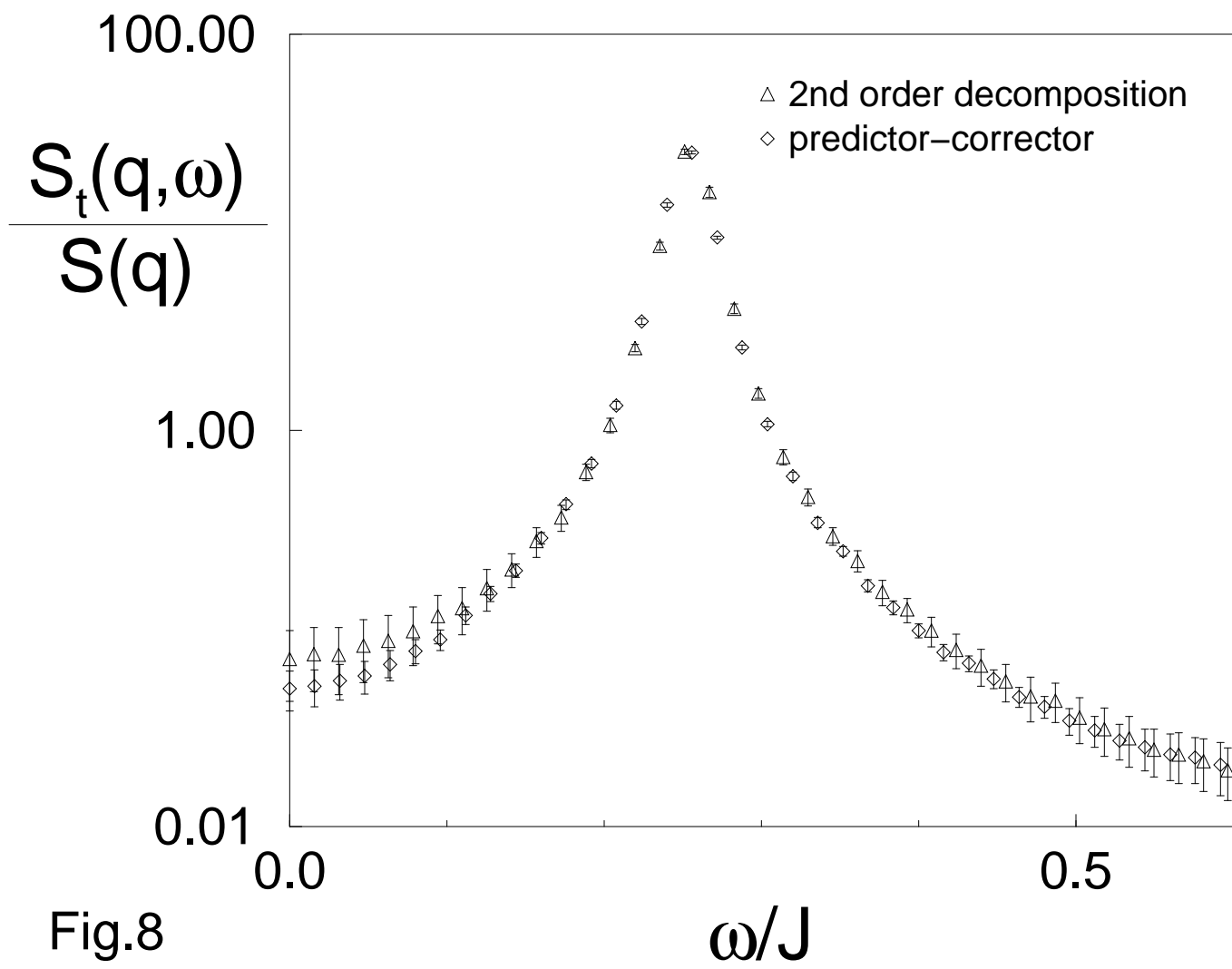


Fig.8